KBr increased more rapidly than that of the 21°K annealing stage. This result suggests that heavier irradiations produce more stable complex forms of interstitial halide ions and that these account for the occurrence of higher temperature annealing stages. It is interesting to note that the concentration of the isolated halide interstitial atoms (the H centers) saturates as a function of radiation dose but that the growth of the H'[14] center is a linear function of the F-center concentration.

[14] B. J. Faraday and W. D. Compton, International Symposium on Color Centers in Alkali Halides, Stuttgart, Germany, 1962 (unpublished).

ACKNOWLEDGMENT

The authors would like to express their deep gratitude to Professor A. Smakula of MIT for supplying them with Cl-doped KBr crystals.

Note added in proof. The authors are grateful to Dr. F. Lüty for bringing to their attention the work of U. Strähle (Diplom, Stuttgart, 1963) in which similar annealing of the α center in Cl-doped KBr is discussed together with an experimental determination of the efficiency of vacancy formation between liquid-helium temperature and 100°K.

PHYSICAL REVIEW VOLUME 138, NUMBER 6A 14 JUNE 1965

Far-Infrared Magnetic Resonance in NiF_2

P. L. RICHARDS
Bell Telephone Laboratories Incorporated, Murray Hill, New Jersey
(Received 22 January 1965)

Measurements of the far-infrared transmission of the canted-spin antiferromagnet NiF_2 using the technique of Fourier-transform spectroscopy are described. Resonant absorptions were found at $\nu_1=3.33\pm0.05$ cm^{-1} and $\nu_2=31.14\pm0.1$ cm^{-1} with applied field $H=0$ and temperature $T\approx0$. Using the resonance relations derived by Joenk and Bozorth from Moriya's model, these give anisotropy and exchange parameters $E=1.66$ cm^{-1} and $8JD=482.2$ cm^{-2}. A good fit is obtained to the measured magnetic-field dependence of both modes for $g_1=2.35$ which, along with the measured perpendicular susceptibility, gives $8J=125$ cm^{-1} and $D=3.86$ cm^{-1}. The temperature dependence of ν_2 was measured between 1.2 and 65°K ($T_N=73.2$°K) and is found to be in agreement with the Zener theory when the temperature dependence of the sublattice magnetization is estimated from neutron-diffraction intensity measurements. The linewidth and strength of mode 2 were also measured as a function of T, and are discussed qualitatively.

I. INTRODUCTION

THE magnetic properties of the iron-group difluorides MnF_2, FeF_2, CoF_2, and NiF_2 have been studied extensively from both an experimental and a theoretical point of view. All these compounds have the rutile crystal structure shown in Fig. 1, and have Néel temperatures T_N between 35 and 75°K, below which magnetic ordering takes place. Susceptibility measurements on MnF_2, FeF_2, and CoF_2 show that the ordering is antiferromagnetic, and neutron-diffraction experiments indicate that the spins point along the $\pm z$ axis.[1] Torque measurements by Mataresse and Stout[2] show that NiF_2, on the other hand, has a weak ferromagnetic moment along a [100] direction. The existence of this moment was explained by Alikhanov,[3] from neutron-diffraction experiments, and by Moriya,[4] from a theoretical interpretation of the torque measurements, in terms of the canted two-sublattice magnetic structure shown in Fig. 2. As was pointed out by Dzialoshinski,[5] and calculated quantitatively by Moriya,[6] there are, in general, two interactions which can cause canted-spin systems. Of these, the antisymmetric exchange coupling,

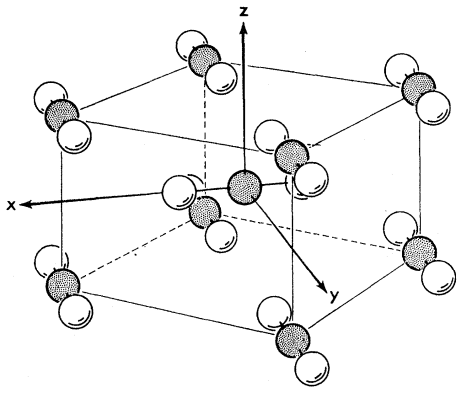

FIG. 1. Rutile-type crystal structure of NiF_2. The solid and open circles represent Ni^{2+} and F^- ions, respectively. It should be noticed that the body-center sites differ from the corner sites only by a rotation of 90° about the z axis.

[1] For a general review, see T. Nagamiya, K. Yoshida, and R. Kubo, Advan. Phys. 4, 1 (1955).
[2] L. M. Matarrese and J. W. Stout, Phys. Rev. 94, 1792 (1954).
[3] A. Alikhanov, Zh. Eksperim. i Teor. Fiz. 37, 1145 (1959) [English transl.: Soviet Phys.—JETP 10, 814 (1960)].
[4] T. Moriya, Phys. Rev. 117, 635 (1960).
[5] I. Dzialoshinski, Zh. Eksperim. i Teor. Fiz. 30, 1454 (1957) [English transl.: Soviet Phys.—JETP 6, 1120 (1958)]; J. Phys. Chem. Solids 4, 241 (1958).
[6] For a recent review, see T. Moriya, in *Magnetism: A Treatise on Modern Theory and Materials*, edited by G. T. Rado and H. Suhl (Academic Press Inc., New York, 1963), Vol. I, Chap. 3.

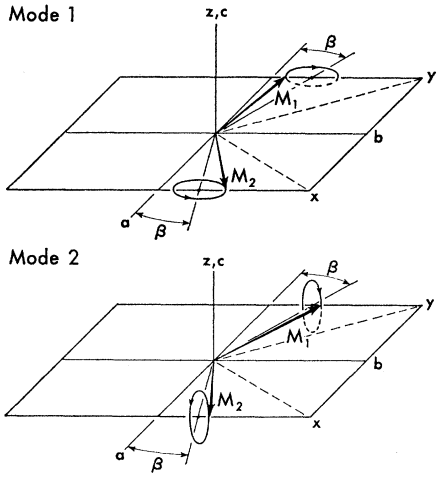

FIG. 2. Zero-field resonant modes 1 and 2. The canting angle $\beta=\eta E/8J\approx 0.38°$ and the widths of the ellipses are exaggerated. The aspect ratios of the ellipses are $\hbar\omega_1/16JS\approx 0.01$ and $\hbar\omega_2/16\sqrt{2}JS\approx 0.088$, respectively.

or Moriya interaction, vanishes by symmetry in NiF_2, but the crystalline field anisotropy in the rutile structure accounts for the canting in a natural way. Two resonant frequencies are expected in such canted-spin systems even in zero external field. Both resonances have been observed in $MnCO_3$, in which canting occurs owing to the Moriya interaction.[7–9] Several authors[4,10,11] have computed the resonant-frequency conditions appropriate for NiF_2. The lower frequency ω_1 is proportional to the anisotropy in the (001) plane and so resembles a ferromagnetic resonance of the net moment. The higher frequency ω_2 is proportional to the geometric mean of the exchange and out-of-plane anisotropy, so is more clearly antiferromagnetic in nature. As is the case for the other iron-group fluorides, these resonances occur at high-microwave and far-infrared frequencies in NiF_2.

In this paper, measurements of the resonant frequencies of NiF_2 using far-infrared techniques are described. The data include the magnetic-field dependence of both ω_1 and ω_2, and the temperature dependence of the frequency, line width, and line strength of mode 2. These measurements, combined with the susceptibility measurements of Joenk and Bozorth,[12] are compared with theory, and values of anisotropy and exchange parameters deduced. A brief account of this work has been given previously.[9,13]

II. THEORY

A summary is presented of the calculation of the resonant properties of NiF_2.[4,10–12] The ground orbital state of Ni^{2+} in NiF_2 lies well below the first excited state, so a spin Hamiltonian can be written in the form

$$\mathcal{H}=J\sum_{j>k}\mathbf{S}_j\cdot\mathbf{S}_k+\sum_j[DS_{jz}^2-E(S_{jx}^2-S_{jy}^2)+\mu_B\mathbf{S}_j\cdot g_j\cdot\mathbf{H}]$$
$$+\sum_k[DS_{kz}^2+E(S_{kx}^2-S_{ky}^2)+\mu_B\mathbf{S}_k\cdot g_k\cdot\mathbf{H}], \quad (1)$$

where j represents a corner site, and k a body-center site, and the coordinate axes are chosen as shown in Fig. 1. The first term is the superexchange interaction, and the second and third terms are the single-ion anisotropy and Zeeman energies of the ions on the two sublattices. g_j and g_k are the g tensors of the Ni^{2+} ions at the corner and body-center sites, respectively. Since $S=1$, there are no higher order terms in the single-ion anisotropy. Equation (1) neglects the exchange interactions within one sublattice (which do not affect the resonant frequencies) and also the anisotropic exchange and magnetic dipole interactions. Moriya[6] has estimated these to be $(\Delta g/g)^2J\sim 0.02J$ and ~ 0.2 cm^{-1}, respectively.

Using a semiclassical approximation, the free energy of N spins can be written as

$$F=\frac{N}{2}[8J\mathbf{S}_j\cdot\mathbf{S}_k+\eta D(S_{jz}^2+S_{kz}^2)$$
$$-\eta E(S_{jx}^2-S_{jy}^2-S_{kx}^2+S_{ky}^2)$$
$$+\mu_B(\mathbf{S}_j\cdot g_j+\mathbf{S}_k\cdot g_k)\cdot\mathbf{H}], \quad (2)$$

where $S_{jz}=S_j\cos\theta$, etc. The factor $\eta=(1-\frac{1}{2}S)$ was introduced by Joenk and Bozorth[12] to correct the classical (large spin) approximation for the quantum-mechanical effects in the anisotropy energy.

The dynamical equations for S_i can be written in the form

$$\dot{\mathbf{S}}_i=-\gamma\mathbf{S}_i\times H_{i\,\mathrm{eff}}, \quad (3)$$

where $\mathbf{H}_{i\,\mathrm{eff}}=-\nabla_{\mathbf{M}_i}F$. Here $\mathbf{M}_i=(N/2)g\mu_B\mathbf{S}_i$ is the moment of the ith sublattice, and $\nabla_{\mathbf{M}_i}$ is the gradient with respect to that moment. The effective fields depend, in general, on the directions of both $\mathbf{M}_1$ and $\mathbf{M}_2$.

The equilibrium positions of $\mathbf{S}_1$ and $\mathbf{S}_2$, determined from Eq. (3) with $\dot{\mathbf{S}}_1=\dot{\mathbf{S}}_2=0$, lie in the (001) plane as is shown in Fig. 2 with canting angle $\beta=E\eta/8J$. The static susceptibilities computed from Eq. (3) are

$$4\chi_{aa}=\chi_{bb}=Ng^2\mu_B^2/16J \quad (4)$$

and

$$\chi_{cc}=(Ng^2\mu_B^2/16J+2D\eta)\approx\chi_{bb}. \quad (5)$$

In the b and c directions, these are the same as $\chi_\perp$ for a conventional antiferromagnet.

In order to calculate the resonant frequencies, the dynamical Eq. (3) must be expressed in terms of deviations from the equilibrium spin positions and linearized by assuming that the deviations are small.

[7] M. Date, J. Phys. Soc. Japan **15**, 2251 (1960).
[8] H. J. Fink and S. Shaltiel, Phys. Rev. **130**, 627 (1963).
[9] P. L. Richards, J. Appl. Phys. **35**, 850 (1964).
[10] G. F. Herrmann, J. Phys. Chem. Solids **24**, 597 (1963).
[11] H. J. Fink, Phys. Rev. **133**, A1322 (1964).
[12] R. J. Joenk and R. M. Bozorth, in Proceedings of the 1964 International Magnetism Conference, Nottingham (to be published).
[13] P. L. Richards, J. Appl. Phys. **34**, 1237 (1963).

The resulting resonant frequencies are

$$(\hbar\omega_1)^2=(4E\eta S)^2+10E\eta Sg_1\mu_BH_b+8JS(g_1-g_2)\mu_BH_b-\frac{(4E\eta Sg_{11}\mu_BH_c)^2}{32JD\eta S^2-12E^2\eta^2S^2}, \quad (6)$$

$$(\hbar\omega_2)^2=32JD\eta S^2+4E^2\eta^2S^2+2E\eta Sg_1\mu_BH_b+8JS(g_1-g_2)\mu_BH_b+\frac{32JD\eta S^2+4E^2\eta^2S^2}{32JD\eta S^2-12E^2\eta^2S^2}(g_{11}\mu_BH_c)^2, \quad (7)$$

where H_b and H_c are the static fields along the b and c axes. The g tensors g_j and g_k have principal axes g_1, g_2, g_{11} and g_2, g_1, g_{11} in the x, y, z coordinate system, and $g_\perp=\frac{1}{2}(g_1+g_2)$. A perturbation calculation gives the g-factor anisotropy $g_1-g_2=4E/|\lambda|$ and $g_\perp-g_{11}=2D/|\lambda|$ in terms of the spin-orbit coupling parameter λ. This small anisotropy has an important effect on the resonance frequencies since (g_1-g_2) enters Eqs. (6) and (7) multiplied by $8J$.[12]

A simple procedure[14] for estimating the strengths of modes 1 and 2 is to use the Kramers-Kronig transform,

$$\chi'(\omega')=\frac{2}{\pi}\int_0^\infty\frac{\omega\chi''(\omega)d\omega}{\omega^2-\omega'^2}, \quad (8)$$

which relates the real and imaginary parts of the susceptibility $\chi(\omega)=\chi'(\omega)-i\chi''(\omega)$. Choosing $\omega'=0$, and assuming a narrow resonant peak in χ'' at ω_0, we have

$$\int_0^\infty\chi''(\omega)d\omega=\tfrac{1}{2}\pi\omega_0\chi'(0). \quad (9)$$

From the phases of the modes pictured in Fig. 2, we see that for mode ω_1 there are net oscillating moments along a and c, while for ω_2 this occurs only along the b axis. Thus, the integrated susceptibilities for rf fields along the a, c, and b directions are $\frac{1}{2}\pi\omega_1\chi_{aa}$, and $\frac{1}{2}\pi\omega_1\chi_{cc}$ for mode 1, and $\frac{1}{2}\pi\omega_2\chi_{bb}$ for mode 2.

If we use the fact that the magnetic absorptions in NiF_2 are weak compared with the lattice absorptions, it can be shown from the theory of the transmission of magnetic insulators that the integrated magnetic absorption strengths $\mathcal{S}=\int\alpha(\nu)d\nu$ in cm^{-2} are $2\omega_0n/c^2$ times the integrated susceptibilities.[15] Here α is the magnetic absorption coefficient, ω_0 the resonant frequency, n the index of refraction at ω_0, and c the velocity of light. Thus, the integrated absorption strengths, in units of cm^{-2}, for rf fields along the a, b, and c directions are

$$\mathcal{S}_a=\pi\omega_1^2n\chi_{aa}/c^2,\qquad \mathcal{S}_c=\pi\omega_1^2n\chi_{cc}/c^2, \quad (10)$$

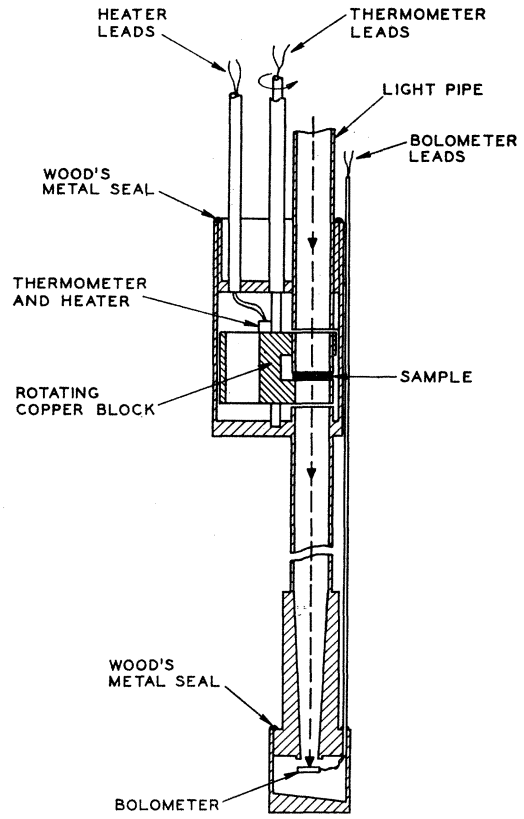

FIG. 3. Sample holder and detector mount for measuring the temperature dependence of sample transmission.

for mode 1, and

$$\mathcal{S}_b=\pi\omega_2^2n\chi_{bb}/c^2 \quad (11)$$

for mode 2.

III. EXPERIMENTAL METHODS

In order to extend the available resolution and frequency range, and to increase the speed of the measurements, the data presented here were obtained by far-infrared Fourier-transform spectroscopy, rather than by using the more conventional diffraction-grating monochromator. With this technique, the interference pattern from a two-beam interferometer is recorded, and the spectrum is obtained by computing the Fourier cosine transform of the interference pattern on a digital computer. The measurements of mode 1 were made primarily with a lamellar-grating interferometer, and these of mode 2 with a Michelson interferometer. Both interferometers, as well as the method of Fourier-transform spectroscopy, have been described fully elsewhere.[16]

The sample holder assembly shown in Fig. 3 was used for measurements of transmission as a function of temperature over the range $1.5<T\lesssim100°K$. A $\frac{1}{2}$-in.-diam evacuated light pipe conveyed the $\sim f/1.4$ radiation from the interferometer into the cryostat, through the

[14] M. Tinkham, Phys. Rev. 124, 311 (1961).
[15] A. J. Sievers, III, thesis, University of California, 1962 (unpublished).
[16] P. L. Richards, J. Opt. Soc. Am. 54, 1474 (1964).

sample, and to the detector. Since the sensitivity of the germanium bolometer detector[16] used for our measurements increased rapidly with decreasing temperature, the whole sample and detector assembly was immersed in liquid helium at ~1.2°K in a conventional glass cryostat.

The sample, an oriented single crystal slab of NiF_2, was glued to a disk of crystalline quartz with rubber cement. Both the sample and the supporting quartz disk were wedge-shaped to reduce interference effects. The quartz disk was in turn cemented to a copper block whose temperature was controlled with a heater and measured with a GaAs diode thermomenter.[17] This thermometer was calibrated in baths of liquid He, H, N, and O. Copper-block temperatures were maintained constant to ±0.3°K by hand adjustment of the heater current. Careful filtering of room-temperature radiation by cooled windows of sooted crystalline quartz maintained the sample temperature within less than 0.3°K of the block temperature.

The sample holder shown in Fig. 3 was designed to permit rotating the sample in and out of the light beam to obtain normalized spectra. In general, however, more useful information on the magnetic absorptions was obtained by comparing spectra obtained above and below T_N, or at different values of magnetic field.

A NbZr superconducting solenoid was used in order to measure sample transmission in magnetic fields up to 50 kOe. It did not prove practical to cool the entire solenoid to the temperature required for bolometer operation, so a small ~1°K helium bath (which was filled by condensation) was used to cool the detector as is shown in Fig. 4. The solenoid and sample were maintained at 4.2°K by a liquid-helium bath at atmospheric pressure. A sample temperature of 4.2°K is sufficiently far below T_N that the field dependence data have essentially their values for $T=0$.

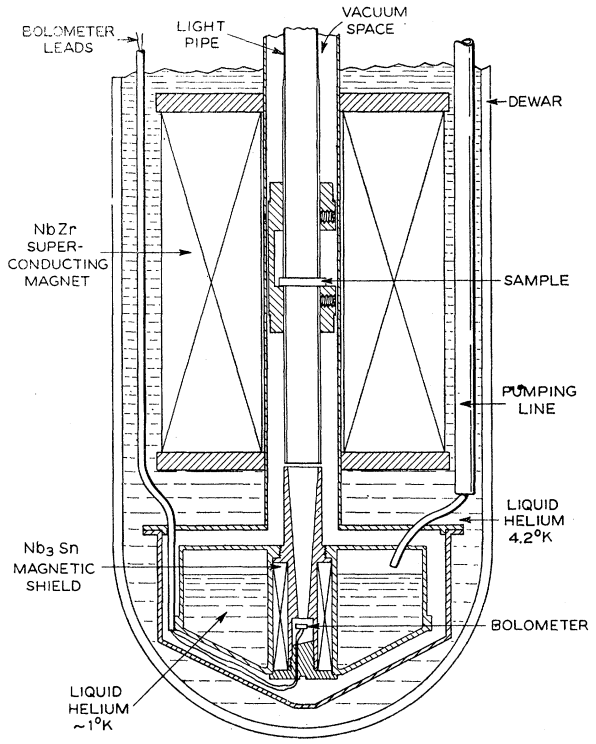

FIG. 4. Sample holder and detector mount for measuring the magnetic-field dependence of sample transmission up to 50 kOe.

[17] B. G. Cohen *et al.*, Rev. Sci. Instr. 34, 1901 (1963).

IV. EXPERIMENTAL RESULTS

Field Dependence of ω_1 and ω_2

Equations (5), (10), and (11) show that the strength of the lower frequency mode ω_1 is reduced by a factor of $\sim(\omega_1/\omega_2)^2$ from that of ω_2. For this reason, the relatively thick (4–7 mm) sample 2 was required to observe ω_1.[18] It was not convenient to orient sample 2 exactly, so the data shown in Fig. 5 were obtained with the static field in the (001) plane, but 12° from the [100] axis.

Moriya[4] has predicted that in zero field NiF_2 is divided into domains parallel to the (001) plane, such that the net moment (b direction) points equally in the [100], [$\bar{1}$00], [010], and [0$\bar{1}$0] directions. Since the sensitivity of our infrared measurements decreased rapidly below ~4 cm^{-1}, we were unable to detect the expected splitting of ω_1 in a small [100] field, but did observe a decreased absorption strength for the lowest field point measured ($H_b\sim2.5$ kOe). The domains align in a [100] field greater than ~5 kOe, and all of the spins see $H_b=H$ (or $H_b=0.978H$ because of the misorientation). Since the measurements were made with unpolarized radiation propagating nearly parallel to H, there is a resonance strength $\sim\mathcal{S}_c$ for one polarization and $\sim\mathcal{S}_a=\frac{1}{4}\mathcal{S}_c$ for the other when H is along a [100] direction.

We were unable to observe mode 1 with a field along the [001] direction. In this orientation the signal is weaker (the strength being $\mathcal{S}_a$ for one polarization, and zero for the other) and the field dependence is negative so that the resonance moves out of the useful range of the spectrometer.

We could not measure mode 1 in zero field, so its frequency was obtained by extrapolating the available data to zero field using the empirical function $\nu_1=(\alpha+\beta H)^M$ cm^{-1} which falls within 0.03 cm^{-1} of the measured points when $\alpha=5.40$, $\beta=0.508$, $M=0.715$, and field H is in kOe. The resulting value of $\nu_1(0)=3.33\pm0.05$ cm^{-1}, along with Eq. (6) and the spin value $S=1$, gives $E=1.66$ cm^{-1}. In order to use Eq. (6) to fit the measured field dependence of ω_1, it is necessary to choose a value for $|\lambda|$ and to estimate $g_1-g_2=4E/|\lambda|$. Using $|\lambda|=250$ cm^{-1} and $g_1=2.35$ we obtain the fit shown in Fig. 5. This g factor is in good agreement with the $g_1=2.33$ obtained from paramagnetic resonance of Ni^{2+} in ZnF_2,[19] and the

[18] Crystal grown by Dr. H. Guggenheim and loaned to the author by Dr. J. Ferguson, Jr.

[19] M. Peter and J. B. Mock, Phys. Rev. 118, 137 (1960).

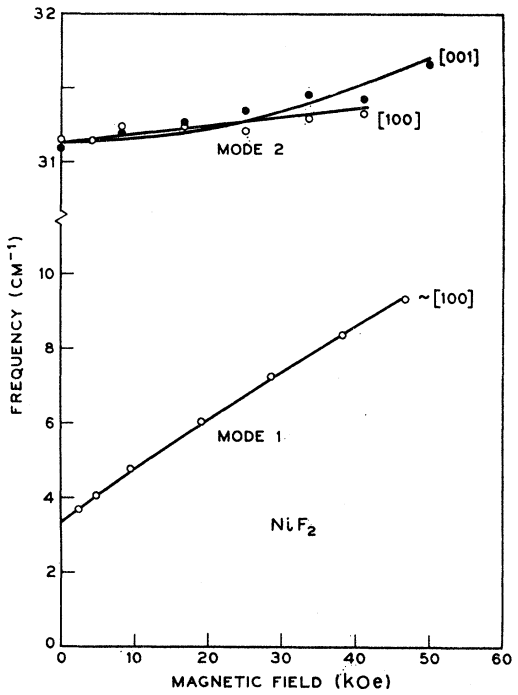

FIG. 5. Magnetic-field dependence of the resonant frequencies ω_1 and ω_2. The frequency scale is different for the two branches. The solid lines are the theoretical predictions with parameters chosen as described in the text.

$g_\perp = 2.32$ obtained from the paramagnetic susceptibility of NiF_2.[12]

Preliminary measurements[13] were made of the higher frequency mode 2 in zero field using an unoriented single crystal plate of irregular shape (sample 1) whose thickness varied between 1.5 and 2.5 mm.[20] Samples 3 and 4, which were in the form of 1–2-mm-thick wedge-shaped plates cut from sample 2 with one face perpendicular to the [001] and [100] axes, respectively, were used for the measurements of the field dependence of mode 2 shown in Fig. 5. For sample 3, with H and radiation propagation along the [001] axis, each polarization should see ω_2 with strength $\mathcal{S}_b \approx 100\mathcal{S}_c$ from half the spins and no contribution from the other half. The observed resonance was considerably stronger than mode 1. In sample 4, with $H<5$ kOe and both field and propagation along [100], the absorption from mode 2 was confined to one polarization, but was otherwise similar to that seen in sample 3. It dropped sharply, however, for higher fields in which the domains were aligned. Only the imperfect collimation of the light and the irregular sample shape, which gave finite components of H_{rf} along the [100] axis, permitted observation of mode 2 in sample 4 when the field was large enough to align the domains.

Averaging the results on the higher frequency mode from samples 1, 3, and 4, gives $\nu_2(0) = 31.14 \pm 0.1$ cm^{-1}. From Eq. (17) we obtain $8JD = 482.2$ cm^{-2}. By using the temperature-dependent portion of susceptibility $\chi_{cc} = 5.75 \times 10^{-3}$ emu/mole[12] and the resonance value of $g_\perp = 2.35$ in Eq. (5), we find $8J = 125$ cm^{-1} and $D = 3.86$ cm^{-1}. It is instructive to compare the anisotropy parameters D and $E = 1.66$ cm^{-1} evaluated from the resonant frequencies and susceptibility of the ordered state with the estimates of the spin Hamiltonian parameters $D = 4.19$ cm^{-1} and $E = 2.67$ cm^{-1} obtained from paramagnetic resonance of Ni^{2+} in ZnF_2.[19]

The field dependences of mode 2 computed from Eq. (7) using the values of g, E, and $8JD$ obtained above, are compared with the experimental points in Fig. 5. The points for a [100] field are fit somewhat better by a line of slope 0.0045 cm^{-1}/kOe, than by the predicted value of 0.0054. The points for an [001] field are fit at least as well by a straight line of slope 0.10 cm^{-1}/kOe as by the quadratic prediction of the theory. The scatter of the data is sufficiently large, however, that neither theoretical curve lies outside the limits of experimental error.

As has been shown by Bozorth *et al.*,[12] the measured net magnetic moment of 161.5 emu/mole is in excellent agreement with the value $N\mu_B SE(g_1\eta/8J_1 + 2/|\lambda|) = 162$ emu/mole computed using the parameters determined from resonance and susceptibility data and assuming that $|\lambda| = 250$ cm^{-1}.

Temperature Dependence of ω_2

The lower frequency ω_1 was not measured at elevated temperatures since it moves out of range of our spectrometer. Measurements were made of $\omega_2(T)$, however, and the results are shown in Fig. 6. These data have an estimated limit of experimental error of ± 0.1 cm^{-1} at low temperatures, increasing with line width to ± 0.6

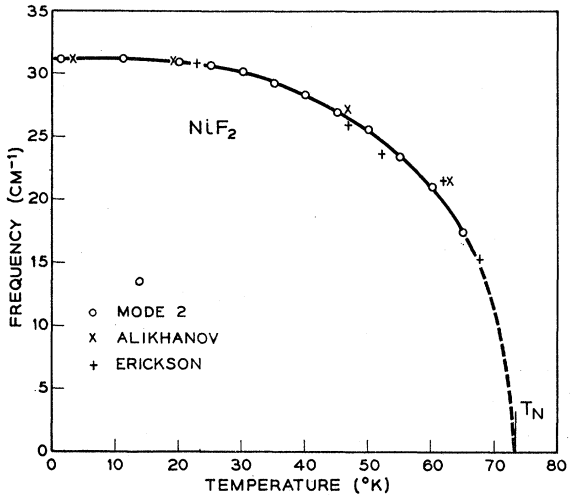

FIG. 6. Temperature dependence of the higher frequency mode 2 in zero magnetic field. The data appear to extrapolate smoothly to zero at T_N, as is expected for antiferromagnetic resonance. The crosses represent the three-fourths power of the temperature dependence of the neutron-diffraction intensities of Erickson and Alikhanov.

[20] Crystal supplied by Dr. R. G. Shulman.

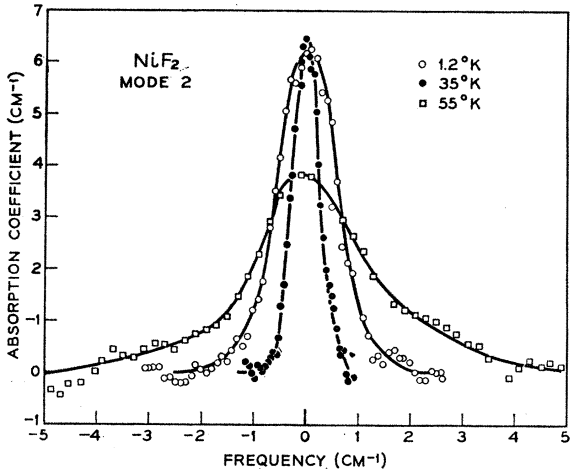

FIG. 7. Temperature dependence of the magnetic absorption coefficient in the neighborhood of the higher frequency mode ω_2. The periodic structure in the wings of the resonance lines is attributed to interference effects, due to multiple reflections in the sample, which are not entirely cancelled by the use of ratios of spectra at different temperatures.

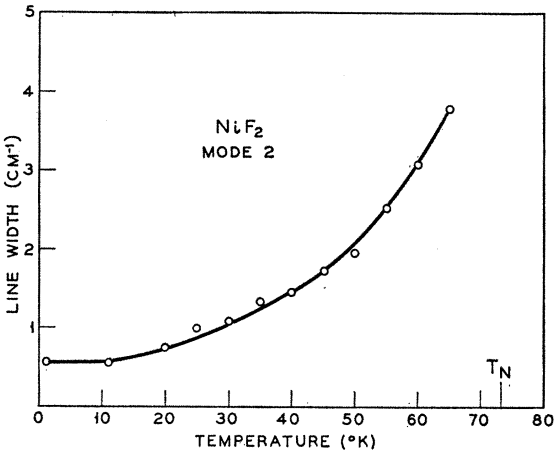

FIG. 8. The temperature dependence of the linewidth of the higher frequency mode.

cm^{-1} for the highest temperature point. The negligible slope of $\omega_2(T)$ at helium temperatures justifies our assumption that measurements at 1.2°K give frequencies corresponding to $T=0$. The similar assumption made for ω_1 should also be valid.

To a good approximation we may write ω_2 in the form of a conventional antiferromagnetic resonance, $\omega_2/\gamma = (2K/\chi_\perp)^{1/2}$, if we let $K=NDS^2$ and $\chi_\perp=\chi_{bb}=\chi_{cc}$. The "perpendicular" susceptibility χ_{cc} is known to be approximately independent of temperature below T_N.[12] According to the Zener theory,[21] the anisotropy constant K is proportional to the third power of the sublattice magnetization. It has been shown[22] for MnO and NiO, and for the iron-group fluorides,[13] that a good fit for $\omega(T)$ can be obtained if the square root of neutron-diffraction-intensity measurements is used to an estimate of the temperature dependence of the sublattice magnetization. The three-fourths powers of the neutron-diffraction points of Erickson[23] and Alikhanov[3] are compared with the measured resonant frequencies in Fig. 6. The accuracy of the neutron data is poor, but the agreement appears to be reasonably good.

Linewidth and Strength of Mode 2

Measurements of the magnetic absorption near ω_2 were made as a function of temperature by computing the ratio of the sample transmission below the Néel temperature to that at $T=80°K>T_N$. Since the magnetic absorptions are weak compared with the lattice absorption, the total reflection from the sample surface is relatively constant near ω_2, and the magnetic absorption coefficient α can be obtained from the negative logarithm of the transmission ratios. Typical data for $\alpha(T)$ in the neighborhood of $\omega_2(T)$ are shown in Fig. 7. These measurements were made on sample 3, which had been cut down to a wedge whose thickness varied from 0.79 to 1.24 mm.

The temperature dependence of the linewidth, defined as the full width when $\alpha=\alpha_{max}/2$, is plotted in Fig. 8. These data have an estimated limit of experimental error of ± 0.1 cm^{-1} for $T<55°K$. At higher temperatures, because of the difficulty of choosing an accurate base line, the errors may be as large as ± 0.3 cm^{-1}. The modest accuracy of our data, and the small range of linewidths covered, make it difficult to distinguish between fluctuation theories of the temperature dependence of the antiferromagnetic linewidth[24,25] and the various mechanisms discussed by Pincus.[26] The width of the line at $T\approx 0$ is not strongly sample-dependent. This result is in agreement with the prediction[26] that impurity and imperfection linewidths in antiferromagnets will be very small compared with 1 cm^{-1}. Only those mechanisms[26] which relax the antiferromagnetic resonance through the optical phonons appear to be capable of producing a linewidth of 0.5 cm^{-1} at $T\approx 0$. This conclusion is supported by the observation that the linewidths of infrared antiferromagnetic resonances at $T\approx 0$ are much larger than those for microwave frequency resonances.[13,23,24,25]

The absorption strength associated with mode 2 was measured by numerically integrating the data for the magnetic absorption coefficient. As can be seen directly from Fig. 7, the line strength appeared to increase nearly linearly with temperature from 4.0 cm^{-2} at 0°K to 14.0 cm^{-2} at 55°K. These data were obtained with unpolarized radiation propagating along the [001] axis

[21] C. Zener, Phys. Rev. **96**, 1335 (1954).
[22] A. J. Sievers, III, and M. Tinkham, Phys. Rev. **129**, 1566 (1963).
[23] R. A. Erickson, Phys. Rev. **90**, 779 (1953).
[24] F. M. Johnson and A. H. Nethercott, Jr., Phys. Rev. **114**, 705 (1959).
[25] R. C. Ohlman and M. Tinkham, Phys. Rev. **123**, 425 (1961).
[26] P. Pincus, J. Phys. Radium **23**, 536 (1962).

of sample 3. Assuming equal numbers of domains of each kind and using the measured index of refraction of $n\sim2.9$ at frequency ω_2, Eq. (11) predicts a strength of 47 cm^{-2} which, like χ_{bb}, should be nearly independent of temperature.

This discrepancy may be analogous to the *apparent* violation of Eq. (9) which occurs for the simple easy-axis antiferromagnets like MnF_2. There $\chi_{\parallel}$ is approximately proportional to T, but no antiferromagnetic resonance absorption is seen when the rf magnetic field is along the c axis. Equation (8) is satisfied (as it must be) by a spread-out region of absorption at higher frequencies which arises from second-order processes.[27]

An alternative explanation of both difficulties could be that the domains were predominanty of one type at low temperatures, but approached a more symmetrical distribution as the temperature increased.

V. CONCLUSIONS

The theory of magnetism in NiF_2 outlined above, originally due to Moriya[4] and extended by Joenk and Bozorth,[12] is adequate for a quantitative description of the measured magnetic-resonance modes of NiF_2. The parameters $E=1.66$ cm^{-1} and $8JD=482.2$ cm^{-2} are obtained directly from the measured frequencies at $T\approx H=0$. We must choose $g_1=2.35$ in order for the theory to fit $\omega_1(H)$. This value is in good agreement with the $g_1=2.32$ and 2.33 obtained from other experiments and adequately predicts $\omega_2(H)$. One further datum is required to separate the exchange parameter $8J=125$ cm^{-1} from the out-of-plane anisotropy $D=3.86$ cm^{-1}. This can be either the susceptibility $\chi_{bb}=\chi_{cc}$ or the net ferromagnetic moment M. The quantitative agreement with the theory is most clearly indicated by the fact that these two approaches lead to values of $8J$ and D which agree within a few percent.

[27] T. Nakamura, Progr. Theoret. Phys. (Kyoto) 7, 539 (1952).

ACKNOWLEDGMENTS

The author is indebted to Dr. R. G. Shulman and Dr. J. Ferguson, Jr., for supplying samples for these measurements, and to Dr. B. Cohen for furnishing the GaAs thermometer. Thanks are also due to A. B. Schaafsma for constructing the magnetic-field apparatus and for assistance with the measurements.

PHYSICAL REVIEW VOLUME 138, NUMBER 6A 14 JUNE 1965

Vibrational Spectra of Lithium-Oxygen and Lithium-Boron Complexes in Silicon

R. M. CHRENKO, R. S. MCDONALD, AND E. M. PELL*
General Electric Research Laboratory, Schenectady, New York
(Received 18 January 1965)

Vibrational spectra of lithium-oxygen and lithium-boron complexes in silicon have been studied using enriched boron and lithium isotopes. The absorption bands in the 300–4000 cm^{-1} region are due to vibrations of interstitial oxygen atoms perturbed by lithium ions, and substitutional boron ions, also perturbed by lithium ions. The 517-cm^{-1} band of interstitial oxygen is displaced to 525 cm^{-1} by Li^7 and to 537 cm^{-1} by Li^6, and the 1106-cm^{-1} band is displaced to 1006 cm^{-1} by both lithium isotopes. (Frequencies are for 78°K except for the 1106- and 1006-cm^{-1} bands which are for 300°K.) No counterpart of the 1203-cm^{-1} band of interstitial oxygen is detected for the lithium-oxygen complex, and on this basis the 1203-cm^{-1} band is reassigned to a combination of the asymmetric SiO stretching vibration with the librational motion of oxygen around the ⟨111⟩ axis rather than to the symmetric SiO stretching fundamental. This new assignment provides a value of 67 cm^{-1} for the frequency of the vibrational mode associated with the libration. The 623-cm^{-1} triply degenerate vibration of isolated substitutional boron ions is split into two bands at 567 and 656 cm^{-1} by interaction with lithium, indicating axial symmetry for the lithium-boron complex. (These frequencies are for the B^{11} isotope.) The precipitation of lithium from the lithium-oxygen complex is inhibited in the presence of boron, probably because in the absence of free electrons the precipitation nuclei develop a positive charge which repels the diffusing lithium species (Li^+).

I. INTRODUCTION

VIBRATIONAL infrared spectra of light impurity atoms in elemental semiconductors which crystallize with the diamond lattice are of interest for many reasons, not the least of which is that the defects seem simple enough to be understood in considerable detail.

The present study was undertaken to learn more about the defect which is formed when dissolved lithium interacts with interstitial oxygen in silicon.

Oxygen forms an uncharged interstitial defect in silicon, the spectrum and chemical behavior of which have been the subject of a number of papers.[1–7] This

* Present address: Xerox Corporation, Rochester, New York.

[1] W. Kaiser, P. H. Keck, and G. F. Lange, Phys. Rev. **101**, 1264 (1956).
[2] H. J. Hrostowski and R. H. Kaiser, Phys. Rev. **107**, 966 (1957).
[3] W. Kaiser, H. L. Frisch, and H. Reiss, Phys. Rev. **112**, 1546 (1958).
[4] H. J. Hrostowski and R. H. Kaiser, J. Phys. Chem. Solids **9**, 215 (1959).
[5] W. L. Bond and W. Kaiser, J. Phys. Chem. Solids **16**, 44 (1960).
[6] H. J. Hrostowski and B. J. Alder, J. Chem. Phys. **33**, 980 (1960).
[7] J. P. Suchet, J. Chem. Phys. **58**, 155 (1961).